View metadata, citation and similar papers at core.ac.uk
brought to you by CORE
provided by Columbia University Academic Commons

© 2013 International Society of Nephrology

OPEN

Expression of HIV transgene aggravates kidney injury in diabetic mice

Sandeep K. Mallipattu[1], Ruijie Liu[1,2], Yifei Zhong[3], Ed Y. Chen[4], Vivette D'Agati[5], Lewis Kaufman[1], Avi Ma'ayan[4], Paul E. Klotman[6], Peter Y. Chuang[1] and John C. He[1,2,4]

[1]Division of Nephrology, Department of Medicine, Mount Sinai School of Medicine, New York, New York, USA; [2]Renal Section, James J. Peters VA Medical Center, New York, New York, USA; [3]Department of Nephrology, Longhua Hospital, Shanghai University of Traditional Chinese Medicine, Shanghai, China; [4]Department of Pharmacology and Systems Therapeutics, Mount Sinai School of Medicine, New York, New York, USA; [5]Department of Pathology, Columbia University, New York, New York, USA and [6]Baylor College of Medicine, Houston, Texas, USA

With the widespread use of combination antiretroviral agents, the incidence of HIV-associated nephropathy has decreased. Currently, HIV-infected patients live much longer and often suffer from comorbidities such as diabetes mellitus. Recent epidemiological studies suggest that concurrent HIV infection and diabetes mellitus may have a synergistic effect on the incidence of chronic kidney disease. To address this, we determined whether HIV-1 transgene expression accelerates diabetic kidney injury using a diabetic HIV-1 transgenic (Tg26) murine model. Diabetes was initially induced with low-dose streptozotocin in both Tg26 and wild-type mice on a C57BL/6 background, which is resistant to classic HIV-associated nephropathy. Although diabetic nephropathy is minimally observed on the C57BL/6 background, diabetic Tg26 mice exhibited a significant increase in glomerular injury compared with nondiabetic Tg26 mice and diabetic wild-type mice. Validation of microarray gene expression analysis from isolated glomeruli showed a significant upregulation of proinflammatory pathways in diabetic Tg26 mice. Thus, our study found that expression of *HIV-1* genes aggravates diabetic kidney disease.

Kidney International (2013) **83,** 626–634; doi:10.1038/ki.2012.445; published online 16 January 2013

KEYWORDS: diabetic nephropathy; glomerulopathy; HIV

Correspondence: *John C. He, Department of Medicine/Nephrology, Mount Sinai School of Medicine, One Gustave L Levy Place, Box 1243, New York, New York 10029, USA. E-mail: cijiang.he@mssm.edu*

Received 16 July 2012; revised 14 September 2012; accepted 18 October 2012; published online 16 January 2013

It had been nearly three decades since the first published reports of HIV-associated nephropathy (HIVAN), an aggressive form of focal segmental glomerulosclerosis in patients with AIDS.[1–3] Within years, HIVAN was recognized not only as an AIDS-defining illness[4] but also as a disease predominant in patients of African descent.[5] The incidence of HIVAN and the progression to end-stage renal disease continued to rise until the advent and use of combination antiretroviral therapy (cART) in the mid 1990s. In fact, with the widespread use of cART, the incidence of end-stage renal disease attributed to HIVAN has reduced to approximately 800–900 cases per year in the United States. However, the prevalence of end-stage renal disease in this population has continued to rise, likely because of an increase in patient survival.[6] In addition, as patients live longer with HIV, they are at increased risk for comorbidities such as hypertension and diabetes mellitus (DM).[7]

Several studies have shown that many patients who undergo a clinically indicated kidney biopsy are diagnosed with a non-HIVAN-related kidney disease in the post-ART era, ranging from immune complex–mediated kidney diseases to arterionephrosclerosis, and diabetic nephropathy.[8–10] Studies such as these suggest that the spectrum of kidney disease has changed considerably in the last 15 years. With this change, the clinical course of kidney disease in the cART era has been more indolent, a slow progressive decline in kidney function with lower levels of proteinuria. Although the Office of AIDS Research Advisory Council has clearly stated in the 2012 guidelines that the presence of HIVAN is an indication for initiation of cART regardless of CD4 count, the decision to start cART in non-HIVAN-related kidney disease independent of other factors remains unclear (Aidsinfo.nih.gov).

Studies have estimated that nearly 15% of HIV-1-infected patients have comorbid DM. In fact, several studies have suggested that concurrent HIV and DM may have an additive effect on the incidence of chronic kidney disease (CKD).[11,12] For example, Choi *et al.*[11] showed that HIV and DM may have a synergistic effect on the incidence of end-stage renal

disease in both Caucasians and African Americans. Specifically, in a recent study using the Veterans Aging Cohort Study database, we demonstrated that concurrent occurrence of HIV and DM has a greater effect on the risk of CKD progression compared with the occurrence of either condition alone.[12]

Since the derivation of the HIV-1 transgenic mice bearing a defective provirus lacking gag-pol (Tg26) in the early 1990s, studies have shown that classical features of HIVAN are exhibited primarily on the FVB background strain.[13] These Tg26 mice at an early age exhibit nephrotic range proteinuria, podocyte dedifferentiation and proliferation, collapsing focal segmental glomerulosclerosis, and microcystic tubular dilatation and injury, consistent with the features observed in HIVAN.[13] However, these changes are not observed in Tg26 mice on the C57BL/6 background. Therefore, Tg26 mice on the C57BL/6 background strain were used to study non-HIVAN kidney disease.

Although epidemiological studies suggest that HIV infection is associated with the progression of CKD in patients with DM, the cause–effect relationship and the mechanism behind this association have yet to be described. Previous studies suggest that chronic inflammation contributes to disease pathogenesis in both diabetic nephropathy and HIVAN.[14,15] Thus, we hypothesized that chronic infection with HIV-1 leads to a proinflammatory state, thereby accelerating diabetic glomerular disease. Here, we demonstrate that streptozotocin (STZ)-induced diabetic mice exhibit more glomerular injury in the presence of HIV-1 transgene expression. We also provide evidence suggesting that this process is associated with an upregulation of proinflammatory pathways.

RESULTS

Diabetic Tg26 mice exhibit an increase in glomerular injury

C57BL/6 mice are typically resistant to STZ-induced diabetic nephropathy[16] and Tg26 mice on the C57BL/6 background are resistant to HIVAN, typically observed on the FVB background.[17,18] To study non-HIVAN-related kidney disease, Tg26 mice on the C57BL/6 background were used to test our hypothesis. To confirm that STZ treatment induced DM in mice, physiological parameters of the mice in each of the four groups were measured (Supplementary Table S1 online). Also, to verify that *HIV-1* viral gene expression was unchanged after induction of diabetes with STZ, *nef* mRNA expression was measured using real-time PCR (Supplementary Figure S1 online). A lack of change in *nef* expression in Tg26 mice with or without diabetes suggests that an increase in glomerular injury observed in diabetic Tg26 mice was not a result of an increase in local viral gene expression. *nef* mRNA expression was undetectable in wild-type (WT) mice (data not shown). At 6 months of age, diabetic Tg26 mice exhibited a significant increase in proteinuria as compared with all other groups (Figure 1). Histological changes by light and electron microscopy at low- and high-power magnification are shown at 6 months of age

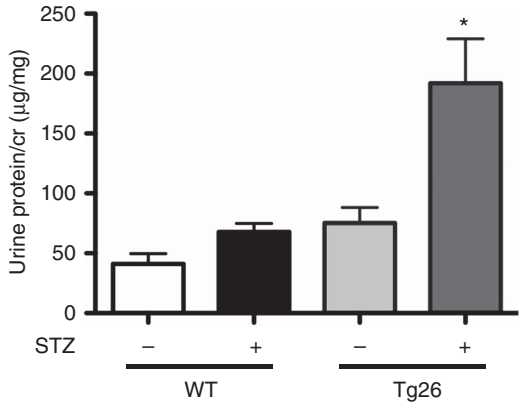

Figure 1 | Diabetic HIV-1 transgenic (Tg26) mice exhibit an increase in proteinuria. Wild-type (WT) and Tg26 mice were treated with streptozotocin (STZ). Urine was collected at baseline before STZ or sodium citrate buffer injection, and the urine protein/creatinine ratio was checked monthly. Urine protein/creatinine ratio at 6 months of age ($n = 6$, $^*P < 0.01$ versus mice treated with sodium citrate buffer).

(Figure 2). Histologically and by quantification, glomerular size, mesangial expansion, and glomerular basement membrane (GBM) thickening were significantly increased in diabetic Tg26 mice compared with all other groups (Figures 3a–c). In addition, diabetic and nondiabetic Tg26 mice had a significant increase in foot process effacement as compared with WT mice with or without diabetes (Figure 3d). Also, the podocyte number per glomerulus was significantly reduced in diabetic Tg26 mice as compared with all other groups (Figure 3e). Combined, these findings suggest that expression of HIV-1 transgene in C57BL/6 diabetic mice induces glomerular injury, typically observed in early diabetic nephropathy.

Increase in the activation of pathways involved in inflammation from enrichment analysis of gene array data in diabetic Tg26 mice

To identify unique or synergistic pathways from the differentially expressed genes in diabetic Tg26 mice, we used oligonucleotide microarrays to profile gene expression in glomeruli isolated from WT mice, diabetic WT mice, Tg26 mice, and diabetic Tg26 mice. Similarly, microarrays from patients with diabetic nephropathy (glomeruli) were retrieved from the Woroniecka Database in Nephromine (http://www.nephromine.org). Also, to compare changes in gene expression in known murine models of diabetic nephropathy, we acquired microarrays deposited in Gene Expression Omnibus (GSE710).[19] For the differentially expressed genes in each experimental group, we performed gene enrichment analysis using the Expression2Kinases software (www.maayanlab.net/X2K/) program to identify pathways involved in inflammation and fibrosis. A combination of gene-list libraries such as Wikipathway, MGI Mammalian Phenotype, KEGG Pathway, and GO molecular function revealed a significant increase in the activation of pathways involving inflammation in diabetic Tg26 mice,

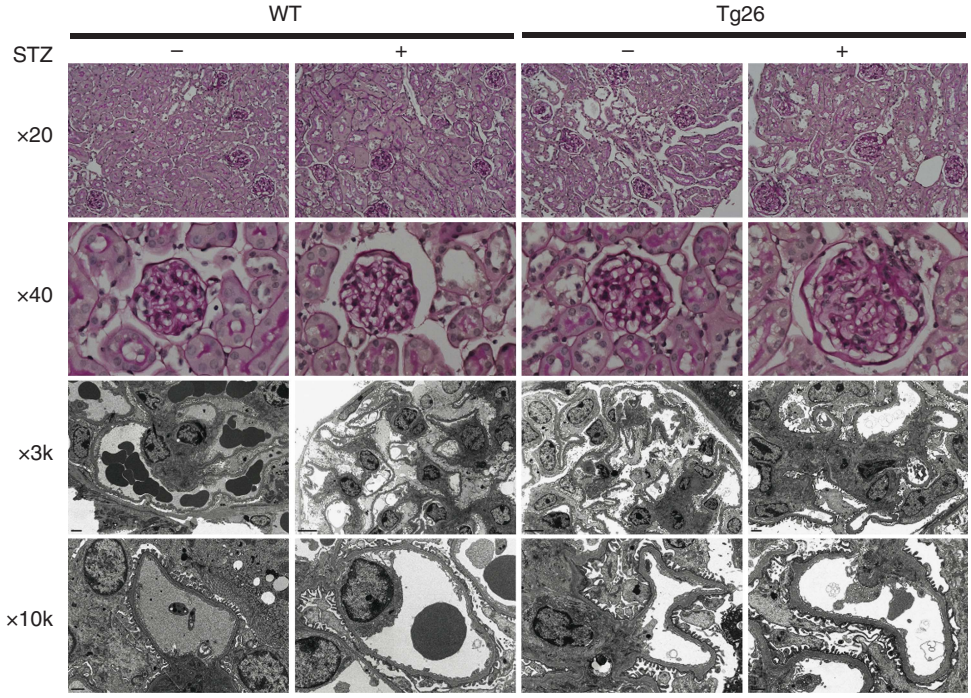

Figure 2 | Diabetic HIV-1 transgenic (Tg26) mice exhibit an increase in glomerular injury. Paraffin-embedded sections were stained with periodic acid–Schiff (PAS) and images were taken at low power (×20) and high power (×40). Ultrastructural changes are shown at low power (×3000) and high power (×10,000) by transmission electron microscopy.

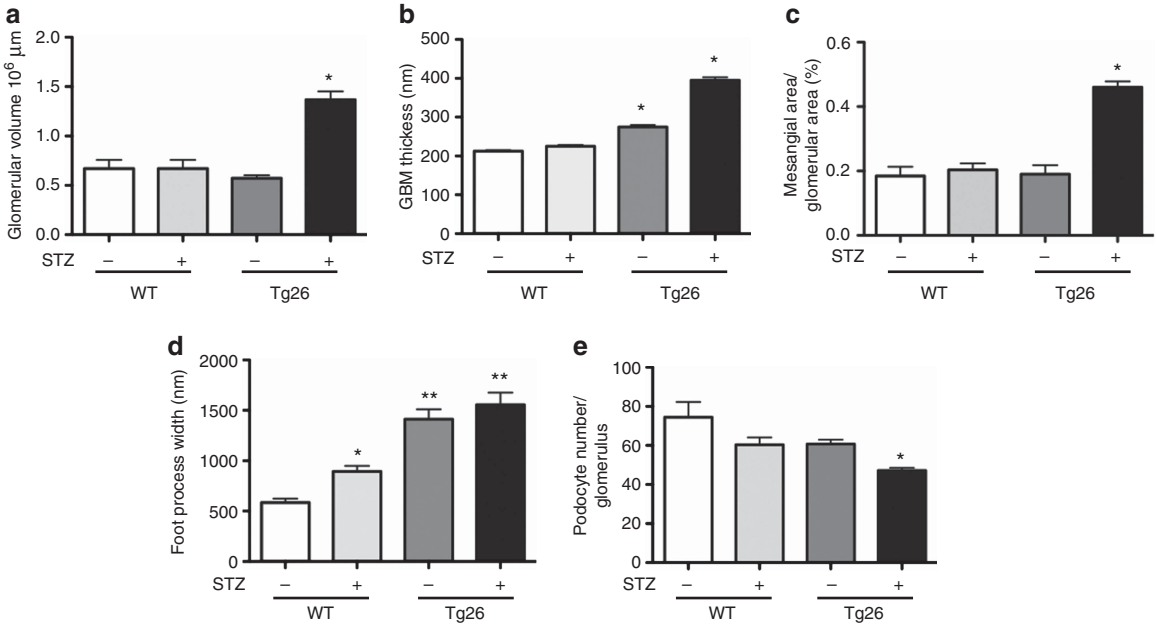

Figure 3 | Quantification of glomerular injury in diabetic HIV-1 transgenic (Tg26) mice. Quantification of (**a**) glomerular volume, (**b**) glomerular basement membrane (GBM) thickness, (**c**) and mesangial expansion is shown ($n = 3$, $^*P < 0.0001$ versus all other groups). (**d**) Quantification of podocyte effacement is shown ($n = 4$, $^*P < 0.0001$ versus all groups, $^{**}P < 0.0001$ versus diabetic and nondiabetic wild-type (WT) mice). (**e**) Quantification of podocyte number is shown ($n = 3$, $^*P < 0.0001$ versus all groups).

consistent with those observed in human diabetic nephropathy and a known murine model of diabetic nephropathy (db/db mice) (Figure 4). These findings suggest that HIV-1 and diabetes may have a synergic effect on the induction of a proinflammatory state leading to the pathogenesis observed in diabetic Tg26 mice.

Upregulation of proinflammatory genes is validated by real-time PCR

To validate the activation of proinflammatory pathways from gene enrichment analysis, primers for selected genes implicated in inflammation were designed (Supplementary Table S2 online) and quantitative real-time PCR was

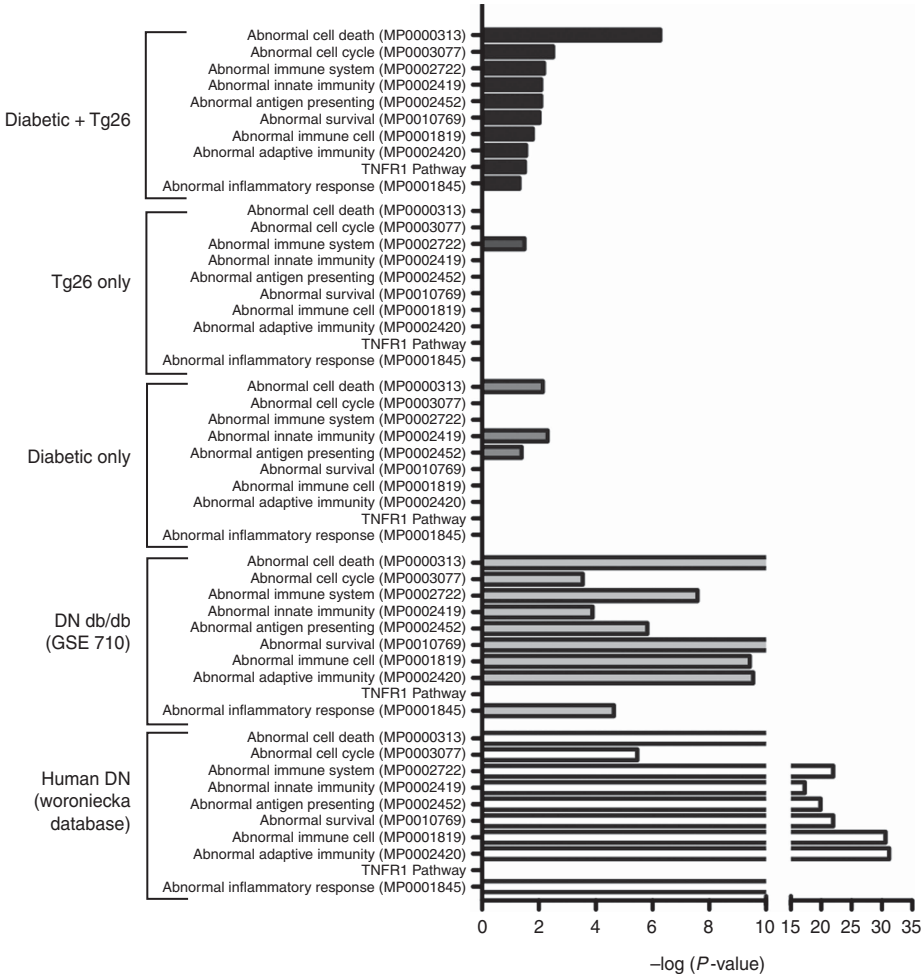

Figure 4 | Activation of pathways involved in inflammation from gene enrichment analysis in diabetic HIV-1 transgenic (Tg26) mice, db/db mice (GSE710), and human diabetic nephropathy. Analysis of terms that are overrepresented among differentially expressed genes in each of the groups as compared with untreated wild-type (WT) mice using a combination of the following gene-list libraries: Wikipathway, MGI Mammalian phenotype, KEGG Pathway, and GO molecular function ($P<0.05$ + Benjamini–Hochberg correction).

performed. These proinflammatory genes include *VCAM1*, *FAS*, *FASL*, *c-MYC*, *CCL2*, and *ICAM1*. Real-time PCR revealed a significant increase in these proinflammatory genes in isolated glomeruli of diabetic Tg26 mice as compared with all other groups (Figure 5). Combined, these findings confirm that a local proinflammatory state is associated with the glomerular disease observed in diabetic Tg26 mice.

Circulating levels of inflammatory markers

To clarify the role of circulating inflammatory markers in the progression of kidney disease observed in diabetic Tg26 mice, serum was collected from all four groups of mice at the time that they were being killed. The sandwich enzyme immunoassay technique was used to measure the circulating levels of TNFR1, TNFR2, and IL-6. A significant increase in TNFR1 and IL-6 serum levels was observed in diabetic-only, Tg26-only, and diabetic Tg26 mice as compared with WT mice (Figures 6a, c). This finding was not observed in circulating levels of TNFR2 (Figure 6b). Although the activation of local inflammatory genes is predominantly observed in diabetic Tg26 mice, elevation of circulating inflammatory cytokines may still contribute to the glomerular changes observed in this group.

Upregulation of profibrotic genes in diabetic Tg26 mice by real-time PCR

To assess for the activation of profibrotic pathways, primers for genes involved in mesangial expansion were designed (Supplementary Table S2 online) and quantitative real-time PCR was performed. These genes include *TGFβ1*, *CTGF*, *Collagen Type I*, and *α-SMA*. Real-time PCR from glomerular extracts revealed a significant increase in the mRNA expression of these genes in diabetic Tg26 mice as compared with all other groups (Figure 7).

Collagen Type IV expression is increased in diabetic Tg26 mice

Collagen Type IV is constitutively expressed in the GBM and in the mesangial matrix.[20] As we observed an increase in GBM thickness and mesangial matrix in diabetic Tg26 mice,

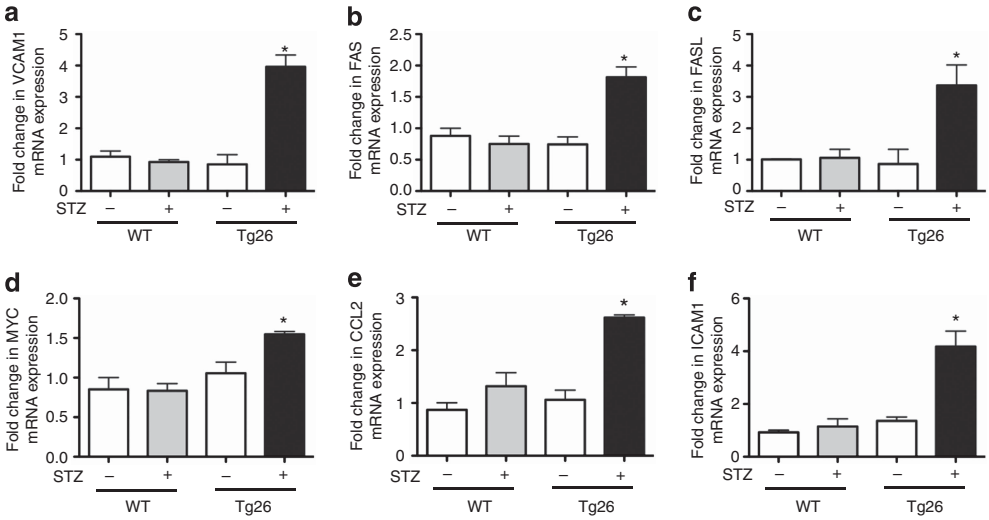

Figure 5 | Upregulation of proinflammatory genes in diabetic HIV-1 transgenic (Tg26) mice is validated by real-time PCR. Glomeruli were isolated from all groups of mice and total RNA was extracted. Real-time PCR was performed for (**a**) VCAM1, (**b**) FAS, (**c**) FASL, (**d**) c-MYC, (**e**) CCL2, and (**f**) ICAM1 ($n = 3$, $^*P < 0.01$ versus all other groups).

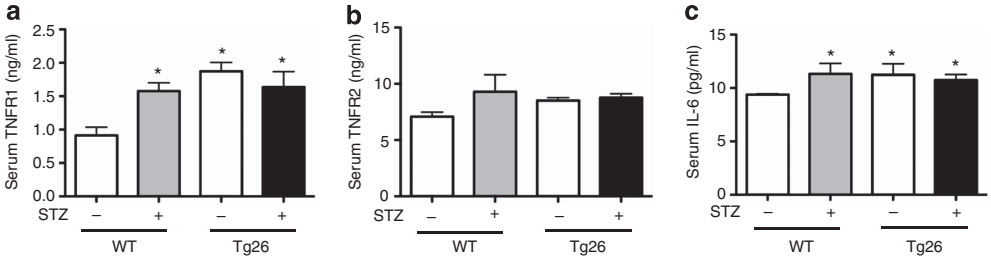

Figure 6 | Measurement of circulating serum inflammatory markers. Blood was drawn and serum was isolated from all groups of mice. The quantitative sandwich enzyme immunoassay was used to measure serum (**a**) tumor necrosis factor receptor 1 (TNFR1), (**b**) tumor necrosis factor receptor 2 (TNFR2), and (**c**) interleukin 6 (IL-6) levels ($n = 6$, $^*P < 0.005$ versus wild-type (WT) mice).

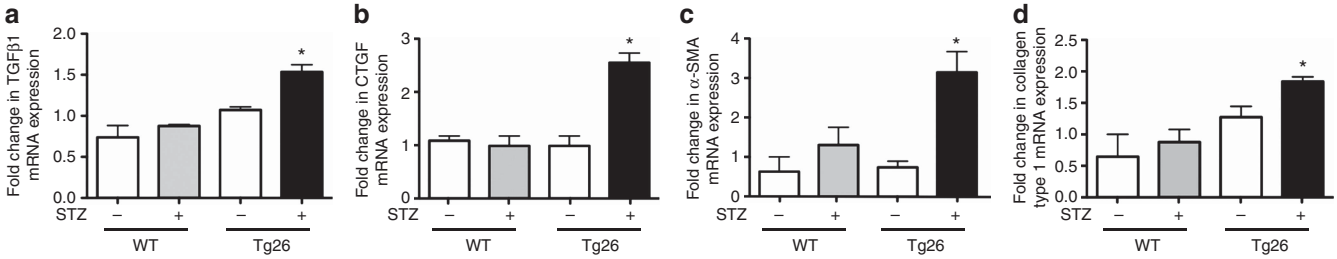

Figure 7 | Upregulation of profibrotic genes in diabetic HIV-1 transgenic (Tg26) mice by real-time PCR. Glomeruli were isolated from all groups of mice and total RNA was extracted. Real-time PCR was performed for (**a**) transforming growth factor beta 1 (TGFβ1), (**b**) connective tissue growth factor (CTGF), (**c**) alpha smooth muscle actin (α-SMA), and (**d**) Collagen Type I ($n = 3$, $^*P < 0.01$ versus all other groups).

Type IV collagen expression was measured to assess for changes in expression and distribution. In isolated glomeruli, Collagen Type IV mRNA expression was significantly increased in diabetic Tg26 mice (Figure 8a). These findings were validated by immunofluorescence qualitatively and quantitatively (Figures 8b and c).

Smad3 phosphorylation is increased in diabetic Tg26 mice

Since there was an upregulation of local profibrotic genes involved in matrix expansion and GBM thickening, we assessed for activation of the TGFβ pathway by measuring Smad3 phosphorylation from the isolated renal cortex. Smad3 phosphorylation was significantly increased in diabetic Tg26 mice (Figure 9a). These findings were quantified by densitometric analysis (Figure 9b). Combined, these findings suggest a significant activation of the profibrotic pathway in diabetic Tg26 mice.

DISCUSSION

A large body of epidemiological studies indicates that the spectrum of HIV-related kidney disease has changed markedly in the last decade. Further, as patients with HIV live longer, they are more susceptible to non-HIVAN-related kidney diseases such as diabetic nephropathy. Although a

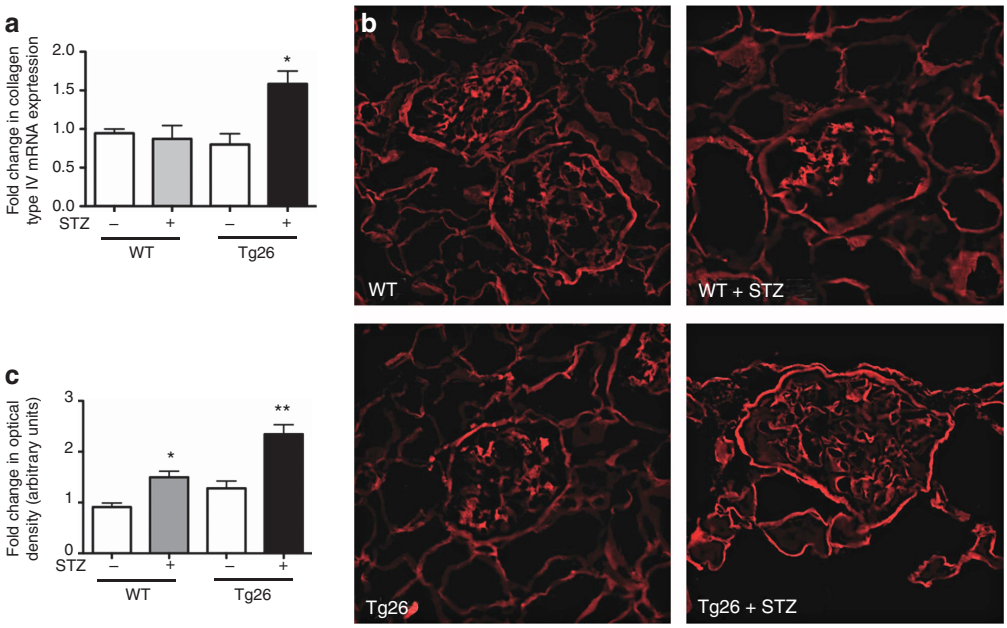

Figure 8 | Collagen Type IV expression is increased in diabetic HIV-1 transgenic (Tg26) mice. Glomeruli were isolated from all groups of mice and total RNA was extracted. (**a**) Real-time PCR was performed for Collagen Type IV ($n = 3$, $^*P < 0.05$ versus all other groups). The renal cortex was isolated from all groups of mice and (**b**) immunofluorescence staining was performed for Collagen Type IV with (**c**) quantification using ImageJ ($n = 3$, $^*P < 0.05$ versus wild-type (WT), $^{**}P < 0.05$ versus all other groups).

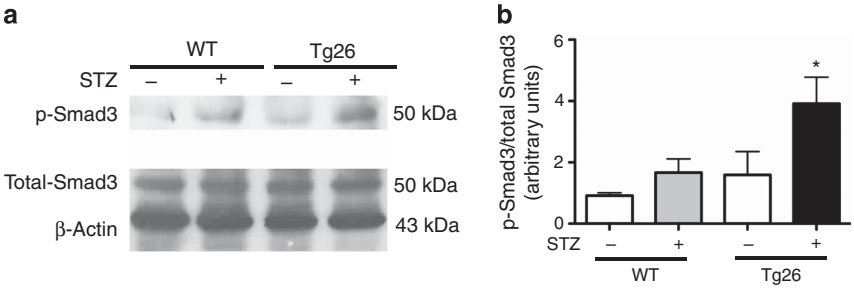

Figure 9 | Smad3 phosphorylation is increased in diabetic HIV-1 transgenic (Tg26) mice. The nuclear protein was initially isolated from the renal cortex and p-Smad3 (Smad3 phosphorylation), total-Smad3, and beta-actin protein expression levels were measured by (**a**) western blot. The representative blots of three independent experiments are shown. (**b**) The densitometric analyses of these blots are shown ($n = 3$, $^*P < 0.05$ versus all other groups).

diagnosis of HIVAN is an indication for cART initiation regardless of CD4 count, it remains unclear whether this remains applicable to patients with non-HIVAN-related kidney disease. Further, mechanisms that contribute to this disease process have yet to be described. Here, we provide evidence that HIV-1 may contribute to or aggravate early stages of glomerular disease observed in diabetic nephropathy probably through activation of proinflammation pathways.

Although epidemiological studies suggest that HIV infection is associated with the progression of diabetic nephropathy, the cause–effect relationship remains unclear. We provide direct evidence showing that expression of HIV-1 transgene in diabetic mice contributes to a significant increase in glomerular injury, mimicking early diabetic nephropathy. The observed changes in glomerular injury in the diabetic Tg26 mice were on the C57BL/6 background, a strain typically resistant to diabetic nephropathy and HIVAN.[16–18] Although these findings suggest that HIV infection contributes to the acceleration of diabetic nephropathy, we acknowledge that the pathology is not overwhelming. In fact, these findings are more representative of an early stage of glomerular disease and are likely attributable to the sclerosis-resistant mouse background, C57BL/6.[21] Diabetes-related glomerulosclerosis is typically observed in sclerosis-prone genetic backgrounds.[16,22,23] Further studies using a similar approach in sclerosis-prone genetic backgrounds will be required to determine the progression to advanced glomerulosclerosis. Nevertheless, we believe that the changes observed in this study are unique and likely attributable to the presence of concomitant diabetes and HIV-1 transgene expression, especially as these pathological changes are typically not observed on this background.

To identify genes or synergistic pathways that have a role in the disease progression observed in diabetic Tg26 mice, microarray expression studies were performed. Using the gene enrichment analysis tool from the Expression2Kinases software,[24] we confirmed that proinflammatory genes were significantly upregulated in diabetic Tg26 mice, suggesting an underlying mechanism mediating the observed disease process. Similar inflammatory pathways were also activated in human diabetic nephropathy as well as in a known murine model of diabetic nephropathy. This suggests that diabetic nephropathy may in part be activated by complementing these inflammatory pathways in C57BL/6 mice in the setting of concomitant diabetes and HIV-1 transgene expression. Also, the activation of inflammatory pathways with HIV infection is consistent with previous studies.[25] Further, HIV-associated inflammation has been implicated in premature onset of other end-organ abnormalities.[25,26] Finally, we observed an upregulation of genes involved in GBM thickening and mesangial expansion, as well as the activation of the TGFβ pathway, in diabetic Tg26 mice. Therefore, we speculate that a state of local chronic inflammation induced by HIV accelerates diabetic kidney disease.

Circulating levels of TNFR1 have been associated with the progression of diabetic nephropathy.[27,28] Minimal, yet significant, elevation in serum TNFR1 and IL-6 may contribute to the early glomerular changes observed in diabetic Tg26 mice. However, it is likely not primarily responsible for the histological changes observed in the diabetic Tg26 mice, as a significant increase in serum TNFR1 and IL-6 levels was also observed in diabetic-only and Tg26-only mice. The role of HIV-induced systemic inflammatory response in kidney injury still remains to be defined until other circulating inflammatory markers are measured. However, in HIVAN, reciprocal renal transplantation between WT and Tg26 mice revealed that intrarenal expression of HIV-1 genes, not systemic inflammation, is responsible for progression to HIVAN.[29] Therefore, the kidney has been considered a reservoir for HIV-1. In this study, a lack of change in *nef* expression in Tg26 mice with or without diabetes suggests that an increase in glomerular injury observed in diabetic Tg26 mice is not a result of an increase in local viral gene expression.

In summary, we report a murine model to study non-HIVAN-related kidney disease. Our studies suggest that the presence of the HIV-1 transgene accelerates the progression of diabetic nephropathy. Further, the activation of local proinflammatory pathways in the setting of concurrent diabetes and HIV-1 transgene expression may contribute to the glomerular injury observed in this murine model. This study provides a novel insight into the potential mechanisms involved in the progression of non-HIVAN-related kidney disease.

MATERIALS AND METHODS

Genotyping of Tg26 mice

The Mount Sinai School of Medicine Animal Institute Committee approved all animal studies, and the NIH Guide for the Care and Use of Laboratory Animals was followed strictly. Derivation of a transgenic mouse line (Tg26 mice) that bears a defective HIV-1 provirus lacking gag-pol (Tg26) has been described.[13] Tg26 mice in the FVB/N background were backcrossed six generations to a C57BL/6 background. WT mice generated from the same litter of Tg26 mice were used as controls in the studies. Genotyping by tail prep and PCR was performed at 2 weeks of age as previously described.[30]

Low-dose STZ-induced diabetes

Induction of diabetes using STZ has been described previously.[31] Briefly, on day 1, Tg26 and WT mice at 6 weeks of age were initially deprived of food for 4 hours. Thereafter, low-dose STZ (50 mg/kg) in 50 mmol/l sodium citrate buffer (pH 5.4) was administered intraperitoneally. STZ was administered similarly at the same dose on days 2–5. On day 14, all mice were deprived of food for 6 h and fasting blood glucose level from the tail vein was checked using the One Touch Blood Glucose Monitoring System. Repeat fasting blood glucose measurements were taken monthly to verify hyperglycemia. Diabetes mellitus was defined as sustained fasting blood glucose above 250 mg/dl at two distinct time points 2 weeks post STZ injection.[31] All mice were killed at 6 months of age.

Measurement of urine albumin and creatinine

Urine albumin was quantified by ELISA using a kit from Bethyl Laboratory (Houston, TX). Urine creatinine levels were measured in the same samples using the QuantiChrom Creatinine Assay Kit (DICT-500) (BioAssay Systems, Hayward, CA) according to the manufacturer's instructions. The urine albumin excretion rate was expressed as the ratio of albumin to creatinine.

Bright-field light microscopy and morphometric studies

Mice were perfused with Hank's buffered salt solution (HBSS) and fixed with 4% paraformaldehyde overnight. Kidney tissue was embedded in paraffin by American Histolabs (Gaithersburg, MD) and 3 μm-thick sections were stained with periodic acid–Schiff (Sigma, St Louis, MO).

Estimation of glomerular volume and mesangial area was made as previously described.[32,33] Briefly, digitized images were scanned and profile areas were traced using ImageJ. The mean glomerular tuft volume was determined from the mean glomerular cross-sectional area by light microscopy. The glomerular cross-sectional area was calculated on the basis of the average area of 30 glomeruli in each group, and glomerular tuft volume was calculated using the following equation:

$$\mathrm{GV} = \frac{\beta}{\kappa} \times \mathrm{GA}^{3/2}$$

($\beta = 1.38$, the shape coefficient of spheres (the idealized shape of glomeruli), and $\kappa = 1.1$, the size distribution coefficient). Also, mesangial expansion was defined as a periodic acid–Schiff-positive and nuclei-free area in the mesangium. Quantification of mesangial expansion was based on 20 glomeruli cut at the vascular pole in each group.

Quantification of podocyte number per glomerulus was determined using Wilm's tumor-1-stained podocytes. First, kidney sections from these mice were prepared in an identical manner. Thereafter, 4 μm-thick sections were stained with rabbit anti-WT-1 (Novus, Littleton, CO) as previously described.[34] Counting of podocytes and quantification of glomerular area and volume were performed using ImageJ and by the method standardized by Animal Models of Diabetic Complications Consortium.[32]

Transmission electron microscopy and morphometric studies

Mice were perfused with HBSS and immediately fixed in 2.5% glutaraldehyde for electron microscopy. Sections were mounted on a copper grid and photographed under a Hitachi H7650 microscope (Tokyo, Japan).

Quantification of podocyte effacement was performed as previously described.[35] Briefly, negatives were digitized, and images with a final magnitude of approximately X15,000 were obtained. ImageJ 1.26t software (National Institute of Health, rsb.info.nih.gov/ij) was used to measure the length of the peripheral GBM, and the number of slit pores overlying this GBM length was counted. The arithmetic mean of the foot process width (W_{FP}) was calculated as follows:

$$W_{FP} = \frac{\pi}{4} \times \frac{\sum \text{GBM length}}{\sum \text{slits}}$$

(Σslits indicates the total number of slits counted, ΣGBM length indicates the total GBM length measured in one glomerulus, and $\pi/4$ is the correction factor for the random orientation by which the foot processes were sectioned).[35]

Sections stained with uranyl acetate and lead citrate were mounted on a copper grid and photographed under a JEOL 1011 transmission electron microscope using Gatan imaging software (Gatan, Warrendale, PA). Quantification of GBM thickness was performed as previously described.[36] The thickness of multiple capillaries was measured in 6–8 glomeruli per mouse ($n = 3$ per group). A mean of 114 measurements was taken per mouse (from podocyte to endothelial cell membrane) at random sites where GBM was displayed in the best cross-section.

Microarray gene expression and gene ontology analysis

Gene expression profiling using Illumina (San Diego, CA) gene expression beadchips was performed at the Mount Sinai Institution Microarray Core Facility. The Illumina MouseWG-6 v2.0 was used to profile gene expression in the glomeruli from all four experimental groups: WT mice, diabetic-only mice, Tg26-only mice, and diabetic Tg26 mice. In brief, the raw data were processed using a Python program in which quantile normalization was performed. The unpaired *t*-test was used to assess statistical significance between the groups. A list of differentially expressed genes was generated for each group using a cutoff of $P < 0.05$ with the Benjamini–Hochberg correction. Enrichment analysis was performed using the Expression2-Kinases software, and Fisher's exact test was used to determine the terms that were overrepresented among the differentially expressed genes in each of the groups compared with untreated WT mice.[24]

Isolation of glomeruli from mice for RNA extraction

Mouse glomeruli were isolated as described.[37] In brief, animals were perfused with HBSS containing 2.5 mg/ml iron oxide and 1% bovine serum albumin. At the end of perfusion, kidneys were removed, decapsulated, minced into 1-mm^3 pieces, and digested in HBSS containing 1 mg/ml collagenase A and 100 U/ml deoxyribonuclease I. Digested tissue was then passed through a 100-μm cell strainer and collected by centrifugation. The pellet was resuspended in 2 ml of HBSS and glomeruli were collected using a magnet. The purity of the glomeruli was verified by microscopy. Total RNA was isolated from kidney glomeruli of mice using TRIzol (Invitrogen, Grand Island, NY).

Real-time PCR

Total RNA was extracted using TRIzol (GIBCO Life Technology, Grand Island, NY). First-strand cDNA was prepared from total RNA (1.5 μg) using the SuperScript III First-Strand Synthesis Kit (Invitrogen), and cDNA (1 μl) was amplified in triplicate using SYBR GreenER qPCR Supermix on an ABI PRISM 7900HT (Applied Biosystems, Foster City, CA). Primers were designed using PrimerBlast (http://www.ncbi.nlm.nih.gov/tools/primer-blast/) and purchased through Sigma (Supplementary Table 2 online), with the exception of previously published primers for *nef* and GAPDH.[7,38] Light cycler analysis software (Carlsbad, CA) was used to determine crossing points using the second derivative method. Efficiency was calculated for all the designed primers using the relative standard curve method. Data were normalized to the housekeeping gene (*GAPDH*) and presented as fold increase compared with RNA isolated from WT animals using the Pfaffl method.[39]

Measurement of inflammation-related serum markers

Initially, 200 μl of blood was collected from mice at the time that they were being killed. Blood samples were allowed to clot for 2 h at room temperature before centrifuging for 20 min at 2000 *g*. Serum was extracted and quantitative sandwich enzyme immunoassay was performed as per manufacturers' protocol to quantify serum TNFR1, TNFR2, and IL-6 levels (no. MRT10, no. MRT20, no. M6000B; R&D systems, Minneapolis, MN).

Immunofluorescence

Kidney sections from these mice were prepared in an identical manner. Immunostaining was performed using rabbit anti-collagen IV (Santa Cruz, Santa Cruz, CA). After washing, sections were incubated with a fluorophore-linked secondary antibody (Alexa Fluor 488 anti-rabbit IgG from Invitrogen). After staining, slides were mounted in Aqua Poly/Mount (Polysciences, Warrington, PA) and photographed under an AxioVision IIe microscope with a digital camera (Munchen, Germany).

Quantification of immunofluorescence

After sections were stained with anti-Collagen Type IV antibody, negatives were digitized, and images with a final magnitude of ~X40 were obtained. ImageJ 1.26t software (National Institute of Health, rsb.info.nih.gov/ij) was used to measure the level of immunostaining in the glomeruli. First, the images were converted to an 8-bit grayscale. Next, the glomerular region was selected for measurement of area and integrated density. Then, the background intensity was measured by selecting three distinct areas in the background with no staining. The corrected optical density was determined as follows:

$$\text{COD} = \text{ID} - (\text{A} \times \text{MGV})$$

(ID is the integrated density of the selected glomerular region; A is the area of the selected glomerular region; and MGV is the mean gray value of the background readings).[40]

Western blot

Glomeruli were lysed with a buffer containing 1% Triton, a protease inhibitor cocktail, and tyrosine and serine-threonine phosphorylation inhibitors. Lysates were subjected to an immunoblot analysis using rabbit anti-phospho Smad3 (Cell Signaling, Danvers, MA), rabbit anti-total Smad3 (Cell Signaling), and mouse anti-β-actin antibodies (Abcam, Cambridge, MA). Densitometric analysis for quantification was performed as previously described.[41]

Statistical analysis

Data were expressed as mean ± s.e.m. ($X \pm$ s.e.m.). The unpaired *t*-test was used to analyze data between two groups. The analysis of

variance followed by Bonferroni's correction was used when more than two groups were present. All experiments were repeated at least three times, and representative experiments are shown. Statistical significance was considered when $P<0.05$.

DISCLOSURE

All the authors declared no competing interests.

ACKNOWLEDGMENTS

We thank Dr A Gharavi for use of the backcrossed Tg26 mice. This work was supported by funds from the NIH/NIDDK (1R01DK078897-01 and 973 fund 2012CB517601 to JCH, P01DK056492 to PEK and JCH, 5K08DK082760 to PYC, and T32 DK07757-12 and 1F32 DK094635-01 to SKM).

SUPPLEMENTARY MATERIAL

Table S1. Physiological parameters of mice treated with and without Streptozotocin (STZ).

Table S2. Oligonucleotide primers used for quantitative real-time PCR analysis.

Figure S1. *nef* expression was unchanged in diabetic and nondiabetic Tg26 mice.

Supplementary material is linked to the online version of the paper at http://www.nature.com/ki

REFERENCES

1. Rao TK, Filippone EJ, Nicastri AD *et al.* Associated focal and segmental glomerulosclerosis in the acquired immunodeficiency syndrome. *N Engl J Med* 1984; **310**: 669–673.
2. Gardenswartz MH, Lerner CW, Seligson GR *et al.* Renal disease in patients with AIDS: a clinicopathologic study. *Clin Nephrol* 1984; **21**: 197–204.
3. Pardo V, Aldana M, Colton RM *et al.* Glomerular lesions in the acquired immunodeficiency syndrome. *Ann Intern Med* 1984; **101**: 429–434.
4. Carbone L, D'Agati V, Cheng JT *et al.* Course and prognosis of human immunodeficiency virus-associated nephropathy. *Am J Med* 1989; **87**: 389–395.
5. Cantor KP, Weiss SH, Goedert JJ *et al.* HTLV-I/II seroprevalence and HIV/HTLV coinfection among U.S. intravenous drug users. *J Acquir Immune Defic Syndr* 1991; **4**: 460–467.
6. Gupta SK, Eustace JA, Winston JA *et al.* Guidelines for the management of chronic kidney disease in HIV-infected patients: recommendations of the HIV Medicine Association of the Infectious Diseases Society of America. *Clinical Infectious Diseases* 2005; **40**: 1559–1585.
7. Mallipattu SK, Wyatt CM, He JC. The new epidemiology of HIV-related kidney disease. *J AIDS Clin Res* 2012; **S4**: 001–006.
8. Berliner AR, Fine DM, Lucas GM *et al.* Observations on a cohort of HIV-infected patients undergoing native renal biopsy. *Am J Nephrol* 2008; **28**: 478–486.
9. Ross MJ, Klotman PE, Winston JA. HIV-associated nephropathy: case study and review of the literature. *AIDS Patient Care STDS* 2000; **14**: 637–645.
10. Fine DM, Perazella MA, Lucas GM *et al.* Kidney biopsy in HIV: beyond HIV-associated nephropathy. *Am J Kidney Dis* 2008; **51**: 504–514.
11. Choi AI, Rodriguez RA, Bacchetti P *et al.* Racial differences in end-stage renal disease rates in HIV infection versus diabetes. *J Am Soc Nephrol* 2007; **18**: 2968–2974.
12. Medapalli R, Parikh CR, Gordon K *et al.* Comorbid diabetes and the risk of progressive chronic kidney disease in HIV-infected adults: Data from the Veterans Aging Cohort Study. *J Acquir Immune Defic Syndr* 2012; **60**: 393–399.
13. Dickie P, Felser J, Eckhaus M *et al.* HIV-associated nephropathy in transgenic mice expressing HIV-1 genes. *Virology* 1991; **185**: 109–119.
14. Fornoni A, Ijaz A, Tejada T *et al.* Role of inflammation in diabetic nephropathy. *Curr Diabetes Rev* 2008; **4**: 10–17.
15. Martinka S, Bruggeman LA. Persistent NF-kappaB activation in renal epithelial cells in a mouse model of HIV-associated nephropathy. *Am J Physiol Renal Physiol* 2006; **290**: F657–F665.
16. Brosius FC 3rd, Alpers CE, Bottinger EP *et al.* Mouse models of diabetic nephropathy. *J Am Soc Nephrol* 2009; **20**: 2503–2512.
17. Zhong J, Zuo Y, Ma J *et al.* Expression of HIV-1 genes in podocytes alone can lead to the full spectrum of HIV-1-associated nephropathy. *Kidney Int* 2005; **68**: 1048–1060.
18. Gharavi AG, Ahmad T, Wong RD *et al.* Mapping a locus for susceptibility to HIV-1-associated nephropathy to mouse chromosome 3. *Proc Natl Acad Sci USA* 2004; **101**: 2488–2493.
19. Susztak K, Bottinger E, Novetsky A *et al.* Molecular profiling of diabetic mouse kidney reveals novel genes linked to glomerular disease. *Diabetes* 2004; **53**: 784–794.
20. Butkowski RJ, Wieslander J, Kleppel M *et al.* Basement membrane collagen in the kidney: regional localization of novel chains related to collagen IV. *Kidney Int* 1989; **35**: 1195–1202.
21. He C, Esposito C, Phillips C *et al.* Dissociation of glomerular hypertrophy, cell proliferation, and glomerulosclerosis in mouse strains heterozygous for a mutation (Os) which induces a 50% reduction in nephron number. *J Clin Invest* 1996; **97**: 1242–1249.
22. Yabuki A, Tanaka S, Matsumoto M *et al.* Morphometric study of gender differences with regard to age-related changes in the C57BL/6 mouse kidney. *Exp Anim* 2006; **55**: 399–404.
23. Yang HC, Zuo Y, Fogo AB. Models of chronic kidney disease. *Drug Discov Today Dis Models* 2010; **7**: 13–19.
24. Chen EY, Xu H, Gordonov S *et al.* Expression2Kinases: mRNA profiling linked to multiple upstream regulatory layers. *Bioinformatics* 2012; **28**: 105–111.
25. Deeks SG. HIV infection, inflammation, immunosenescence, and aging. *Annu Rev Med* 2011; **62**: 141–155.
26. Robertson KR, Smurzynski M, Parsons TD *et al.* The prevalence and incidence of neurocognitive impairment in the HAART era. *AIDS* 2007; **21**: 1915–1921.
27. Shikano M, Sobajima H, Yoshikawa H *et al.* Usefulness of a highly sensitive urinary and serum IL-6 assay in patients with diabetic nephropathy. *Nephron* 2000; **85**: 81–85.
28. Niewczas MA, Gohda T, Skupien J *et al.* Circulating TNF receptors 1 and 2 predict ESRD in type 2 diabetes. *J Am Soc Nephrol* 2012; **23**: 507–515.
29. Bruggeman LA, Dikman S, Meng C *et al.* Nephropathy in human immunodeficiency virus-1 transgenic mice is due to renal transgene expression. *J Clin Invest* 1997; **100**: 84–92.
30. Feng X, Lu TC, Chuang PY *et al.* Reduction of Stat3 activity attenuates HIV-induced kidney injury. *J Am Soc Nephrol* 2009; **20**: 2138–2146.
31. Wu KK, Huan Y. Streptozotocin-induced diabetic models in mice and rats. *Curr Protoc Pharmacol* 2008; **Chapter 5**: Unit 5 47; 5.47.1–5.47.14.
32. Sanden SK, Wiggins JE, Goyal M *et al.* Evaluation of a thick and thin section method for estimation of podocyte number, glomerular volume, and glomerular volume per podocyte in rat kidney with Wilms' tumor-1 protein used as a podocyte nuclear marker. *J Am Soc Nephrol* 2003; **14**: 2484–2493.
33. Awazu M, Omori S, Ishikura K *et al.* The lack of cyclin kinase inhibitor p27(Kip1) ameliorates progression of diabetic nephropathy. *J Am Soc Nephrol* 2003; **14**: 699–708.
34. Schiffer M, Mundel P, Shaw AS *et al.* A novel role for the adaptor molecule CD2-associated protein in transforming growth factor-beta-induced apoptosis. *J Biol Chem* 2004; **279**: 37004–37012.
35. Koop K, Eikmans M, Baelde HJ *et al.* Expression of podocyte-associated molecules in acquired human kidney diseases. *J Am Soc Nephrol* 2003; **14**: 2063–2071.
36. Reiniger N, Lau K, McCalla D *et al.* Deletion of the receptor for advanced glycation end products reduces glomerulosclerosis and preserves renal function in the diabetic OVE26 mouse. *Diabetes* 2010; **59**: 2043–2054.
37. Takemoto M, Asker N, Gerhardt H *et al.* A new method for large scale isolation of kidney glomeruli from mice. *Am J Pathol* 2002; **161**: 799–805.
38. Zuo Y, Matsusaka T, Zhong J *et al.* HIV-1 genes vpr and nef synergistically damage podocytes, leading to glomerulosclerosis. *J Am Soc Nephrol* 2006; **17**: 2832–2843.
39. Pfaffl MW. A new mathematical model for relative quantification in real-time RT-PCR. *Nucleic Acids Res* 2001; **29**: e45.
40. Potapova TA, Sivakumar S, Flynn JN *et al.* Mitotic progression becomes irreversible in prometaphase and collapses when Wee1 and Cdc25 are inhibited. *Mol Biol Cell* 2011; **22**: 1191–1206.
41. Gassmann M, Grenacher B, Rohde B *et al.* Quantifying Western blots: pitfalls of densitometry. *Electrophoresis* 2009; **30**: 1845–1855.

This work is licensed under the Creative Commons Attribution-NonCommercial-No Derivative Works 3.0 Unported License. To view a copy of this license, visit http://creativecommons.org/licenses/by-nc-nd/3.0/